

On the concordance of cosmological data in the case of the generalized Chaplygin gas

R. Aurich and S. Lustig

*Institut für Theoretische Physik, Universität Ulm,
Albert-Einstein-Allee 11, D-89069 Ulm, Germany*

Abstract

The generalized Chaplygin gas cosmology provides a prime example for the class of unified dark matter models, which substitute the two dark components of the standard cosmological Λ CDM concordance model by a single dark component. The equation of state of the generalized Chaplygin gas is characterised by a parameter α such that the standard Λ CDM model is recovered in the case $\alpha = 0$ with respect to the background dynamics and the cosmic microwave background (CMB) statistics. This allows to investigate the concordance of different cosmological data sets with respect to α . We compare the supernova data of the Supernova Cosmology Project, the data of the baryon oscillation spectroscopic survey (BOSS) of the third Sloan digital sky survey (SDSS-III) and the CMB data of the Planck 2015 data release. The importance of the BOSS Lyman α forest BAO measurements is investigated. It is found that these data sets possess a common overlap of the confidence domains only for Chaplygin gas cosmologies very close to the Λ CDM model.

Keywords: dark energy theory, cosmic microwave background, large-scale structure

PACS: 98.80.-k, 98.70.Vc, 98.80.Es

1. Introduction

For almost two decades, cosmology possesses a standard cosmological model which allows a remarkable successful description of a large variety of observational data, the Λ CDM concordance model. For a recent review on the various data sets, see e. g. [1]. Although there is currently no competing cosmological model, there remain tensions [2] which justify the investigation of alternatives. The Λ CDM concordance model is based on two dark ingredients, the dark energy in the form of the cosmological constant Λ and the cold dark matter (CDM). There have ever been attempts to establish alternative cosmological models which are based only on a single dark component, the so-called unified dark matter (UDM) models.

The prototypical model for a UDM cosmology is provided by a dark matter fluid having the equation of state $p = -A/\varepsilon$ of the Chaplygin gas, where ε and

p denote the energy density and the pressure, respectively, and A is a model parameter. The Chaplygin gas was put in a cosmological context by the work of Kamenshchik, Moschella and Pasquier [3] where also an obvious generalisation of the equation of state $p = -A/\varepsilon^\alpha$ with $\alpha > -1$ was introduced. For some further early works on the Chaplygin gas cosmology, see [4–11]. The paper [12] tests the Chaplygin gas against gravitational lenses and age estimations. The generalised Chaplygin model has the nice property that the background cosmology is for $\alpha = 0$ identical to the Λ CDM model. This allows to test how far the equation of state of the dark fluid can deviate from that of the cosmological constant Λ , that is $p = -\varepsilon$. Then, it was discovered [13] that a wide class of UDM cosmologies suffer from instabilities which lead to matter power spectra incompatible with the observations. Especially, it was found in [13] that the generalised Chaplygin gas cosmologies with $|\alpha| \gg 10^{-5}$ are ruled out. Thus, only a minute parameter space of the generalised Chaplygin cosmology was left with values of α so close to zero that these models are almost indistinguishable from the Λ CDM model.

A loophole for the UDM models is already proposed in [13]. It is noted that the dark fluid considered so far does not exploit the full range of physical fluid properties. It is shown in [14] that the fluid is not fully specified by defining the adiabatic speed of sound c_{ad} , but in addition, varying the effective speed of sound c_{eff} and the parameter c_{vis} , as defined in [14], leads to a plethora of behaviours. It is shown in [15] that choosing the effective speed of sound c_{eff} different from the adiabatic one leads to an admissible parameter range of α that is significantly extended. Thus a large class of generalised Chaplygin cosmologies is compatible with the large scale structure and CMB observations, if $c_{\text{eff}} \neq c_{\text{ad}}$ is allowed.

This generated again a large interest in the Chaplygin cosmologies and its variants, see e. g. [16–32]. Most papers assume a flat universe when the allowed parameter space is estimated according to various cosmological data. Assuming a flat universe, the 2σ estimation $\alpha = -0.14_{-0.19}^{+0.30}$ is stated in [20] from a joint analysis of supernovae, BAO, and CMB data. A recent analysis, which also assumes a flat universe, finds the 1σ estimation $\alpha = -0.03_{-0.057}^{+0.067}$ [23]. Both use for their CMB analysis a compressed likelihood which reduces the CMB information to a few numbers among them the shift parameter \mathcal{R} [33, 34]. However, since the matter-like content is not conserved in UDM cosmologies, the shift parameter \mathcal{R} is not strictly applicable in this case. Negative values for α are also found for a flat universe by including gamma-ray bursts data [24], however, the reliability of these data is strongly debated. To be compatible with the rotation curves of galaxies, dark matter haloes consisting of pure generalised Chaplygin gas should satisfy $\alpha \lesssim 0.0001$ [25].

As a modification of the generalised Chaplygin gas, the equation of state $p = \beta\rho - A/\rho^\alpha$ is proposed, but it is found in [26, 27] that β has to be very small. Thus, both the energy density and the equation of state approach those of the generalised Chaplygin gas. Also not exactly comparable, their values for α , that is $\alpha = 0.11_{-0.25}^{+0.34}$ [26] and the 1σ interval $\alpha \in [0.08, 0.31]$ [27], should be of the order of those expected in the generalised Chaplygin gas. Their CMB analysis also makes use of the shift parameter \mathcal{R} .

The generalised Chaplygin gas can also serve as a model for interacting dark matter [28]. Using supernovae data calibrated with different fitters in a joint analysis, even smaller values of α are found in [30], such as $\alpha \simeq -0.5$ or $\alpha \simeq -0.36$, which shows the sensitivity of the chosen calibration method of SNe Ia data. Using additional data sets, a joint analysis carried out in [23] finds the 1σ estimation $\alpha = 0.004_{-0.010}^{+0.013}$. This analysis assumes a flat universe, which is also the case for the recent joint analysis [31] which states $|\alpha| < 0.05$. Although [31] uses the full CMB spectra, their analysis does not vary all cosmological parameters, so that it is not a best-fit analysis. Furthermore, they use the binned JLA supernova data [35], which are strongly dependent on the fiducial Λ CDM model.

It is worthwhile to remark that the correspondence between the generalised Chaplygin gas cosmology for $\alpha = 0$ and the Λ CDM cosmology refers to the background level. On the perturbation level, there are differences but it turns out that the CMB statistics is the same within linear perturbation theory. Since we consider only background data and CMB data in this paper, we equate the generalised Chaplygin gas cosmology for $\alpha = 0$ with the Λ CDM model, but the difference should be kept in mind.

So there is a wide range of possible parameter values and structures for the equation of state. It is the aim of this paper to provide a parameter estimation of the generalised Chaplygin gas cosmology without the restriction to flat universes. Furthermore, the tensions between the different data sets with respect to the Chaplygin gas cosmology are discussed. A special focus is put on the question for which equation of state of the generalised Chaplygin gas a concordance between the supernovae, BAO, and CMB data is achieved. In section 2 the Chaplygin cosmology is introduced, while section 3 states the details about the cosmological data used for the parameter estimation. Section 4 presents the analysis and section 5 concludes with a summary of the results.

2. The generalised Chaplygin gas cosmology

The equation of state of the generalised Chaplygin gas is defined as

$$p = -\frac{A}{\varepsilon^\alpha} \quad (1)$$

with $\alpha > -1$ and A a constant parameter. The original Chaplygin gas is obtained for $\alpha = 1$. The integration of the continuity equation leads to the energy density $\varepsilon_{\text{Chap}}(z)$ of the generalised Chaplygin gas as a function of the redshift z

$$\varepsilon_{\text{Chap}}(z) = \varepsilon_{\text{Chap}}^0 \left\{ (1-B)(z+1)^{3(\alpha+1)+B} \right\}^{1/(\alpha+1)} \quad \text{with } B := \frac{A}{(\varepsilon_{\text{Chap}}^0)^{\alpha+1}} . \quad (2)$$

This leads to the equation of state

$$w_{\text{Chap}}(z) = \frac{p}{\varepsilon} = -\frac{B}{(1-B)(z+1)^{3(\alpha+1)+B}} , \quad (3)$$

which satisfies one of the most important properties of a UDM model: It has to behave matter-like at an early epoch in the history of the universe in order to allow sufficient structure formation, and dark-energy-like at later times in order to explain the accelerated expansion. The generalised Chaplygin gas model has the remarkable property that its background model is for $\alpha = 0$ and $B = 1/(1 + \Omega_{\text{CDM}}/\Omega_{\Lambda})$ identical to that of the Λ CDM concordance model with the same parameters Ω_{CDM} and Ω_{Λ} .

In our analysis we will exclude the parameter space with $B > 1$, since the present equation of state is then $w_{\text{Chap}}(z = 0) = -B < -1$ which corresponds to the so-called phantom energy. But more worse, at the redshift $z = (B/(B - 1))^{1/3(\alpha+1)} - 1 > 0$ the equation of state becomes singular. It will turn out that this restriction is only relevant, if one uses solely the BAO data with $z < 1$ for matching the Chaplygin cosmology.

The effective content of cold dark matter of a UDM model can be computed as argued in [36] by rewriting the evolution of the dark energy density as

$$\begin{aligned} \varepsilon_{\text{de}}(z) &= \varepsilon_{\text{de}}^0 \exp\left(3 \int_{x(z)}^1 \frac{1 + w_{\text{de}}(x)}{x} dx\right) \\ &= \varepsilon_{\text{de}}^{\text{eff}} \left(\frac{a_0}{a(z)}\right)^3 \exp\left(-3 \int_0^{x(z)} \frac{w_{\text{de}}(x)}{x} dx\right) \quad , \end{aligned} \quad (4)$$

where $x := a(z)/a_0$ is the scale factor $a(z)$ normalised to one at the present time and $\varepsilon_{\text{de}}^0$ is the current energy density. Here, we have defined

$$\varepsilon_{\text{de}}^{\text{eff}} := \varepsilon_{\text{de}}^0 \exp\left(3 \int_0^1 \frac{w_{\text{de}}(x)}{x} dx\right) \quad , \quad (5)$$

which converges for an equation of state with $w_{\text{de}}(x) \rightarrow 0$ for $x \rightarrow 0$ as it is the case for UDM models. The quantity $\varepsilon_{\text{de}}^{\text{eff}}$ measures the effective content of cold matter at early times, since the last exponential factor in eq. (4) takes on values close to one at early times.

It is convenient to define the cosmological parameters

$$\Omega_{\text{de}} := \frac{8\pi G}{3H_0^2 c^2} \varepsilon_{\text{de}}^0 \quad \text{and} \quad \Omega_{\text{de}}^{\text{eff}} := \frac{8\pi G}{3H_0^2 c^2} \varepsilon_{\text{de}}^{\text{eff}} \quad (6)$$

with the Hubble constant H_0 and the gravitational constant G . This allows the comparison with the Λ CDM concordance model, where $\Omega_{\text{de}}^{\text{eff}}$ of the UDM model corresponds to the cold dark matter component and $\Omega_{\text{de}} - \Omega_{\text{de}}^{\text{eff}}$ to the effective vacuum energy contribution.

The effective matter density $\Omega_{\text{de}}^{\text{eff}}$ can be computed for the generalised Chaplygin gas model leading to

$$\Omega_{\text{Chap}}^{\text{eff}} = \Omega_{\text{Chap}} (1 - B)^{1/(1+\alpha)} \quad \text{for} \quad \alpha > -1 \quad . \quad (7)$$

This shows that $\Omega_{\text{Chap}} - \Omega_{\text{Chap}}^{\text{eff}}$ becomes negative for $B < 0$, which would correspond in the Λ CDM case to a negative Ω_{Λ} that is an anti-de Sitter like model. We thus restrict the following analysis to $0 < B < 1$ and $\alpha > -1$.

In our analysis, the cosmological model is specified by the total relative density

$$\Omega_{\text{tot}} = \Omega_{\text{rad}} + \Omega_{\text{bar}} + \Omega_{\text{Chap}} \quad . \quad (8)$$

The radiation term Ω_{rad} takes the energy density of photons and neutrinos with standard thermal history into account. The baryon density Ω_{bar} is determined by the choice of the Hubble constant $H_0 = 100 h \text{ km}/(\text{s Mpc})$ as $\Omega_{\text{bar}} = 0.0223/h^2$, so that the physical density of baryons is in agreement with the Big-Bang nucleosynthesis, i. e. according the measured deuterium to hydrogen abundance ratio [37]. As described below, the parameter estimation is carried out with the Markov chains Monte Carlo (MCMC) algorithm and in some selected cases, MCMC sequence are generated with an independently varying $\Omega_{\text{bar}}h^2$ with $\Omega_{\text{bar}}h^2 = 0.0223 \pm 0.0009$. It is found that no change of the parameters defining the Chaplygin gas cosmology α and B occurs. Since every additional parameter leads to longer MCMC sequences until convergence is reached, we do not independently vary this parameter for the further analysis in this paper.

Note, that in equation (8) the dark sector is solely described by the Chaplygin gas component which contrasts to other analyses which add an extra cold dark matter term or a cosmological constant. We have as model parameters the reduced Hubble constant h , which in turn fixes Ω_{bar} , the density Ω_{Chap} together with the parameters α and B , which specify the equation of state (3) of the Chaplygin gas. The background dynamics is determined by

$$H(z) = H_0 \left[\Omega_{\text{rad}}(z+1)^4 + \Omega_{\text{bar}}(z+1)^3 + (1 - \Omega_{\text{tot}})(z+1)^2 + \Omega_{\text{Chap}} \{B + (1-B)(z+1)^{3(1+\alpha)}\}^{1/(1+\alpha)} \right]^{1/2} \quad . \quad (9)$$

3. The cosmological data sets

In this section, we describe the cosmological observations that are used for the estimation of the model parameters discussed in section 2. The parameter estimation is carried out with the Markov chains Monte Carlo (MCMC) algorithm which uses as parameters α and B occurring in the equation of state (1) and (2), the density Ω_{Chap} and the reduced Hubble constant h . In several cases, the parameter α is held fixed so that only B , Ω_{Chap} and h are varied. The probability for selecting a new state in the Markov chain is obtained from the χ_{tot}^2 values

$$\chi_{\text{tot}}^2 = \chi_{\text{Sn}}^2 + \chi_{\text{BAO}}^2 + \chi_{\text{CMB}}^2 \quad , \quad (10)$$

whose individual contributions are discussed below.

In all cases the length of the MCMC sequences is at least 25 000. Several chains are generated and it is checked that they lead to the same confidence contours. Furthermore, the convergence of the Markov chains is checked by computing the MCMC power spectrum and the convergence ratio r along the lines described in [38].

3.1. The supernovae Ia data

The supernovae Ia are now established standard candles whose observed magnitude-redshift dependence can be compared with the theoretical prediction of a given model. We use the Union 2.1 compilation of the Supernova Cosmology Project [39] where the redshift and distance modulus μ_i^{obs} including its uncertainty $\sigma_{i,\text{Sn}}$ for $N_{\text{Sn}} = 580$ supernovae Ia are given. The calibration of the SNe Ia light curves makes use of a fiducial Λ CDM model so this data set possesses a model-dependence and favours the Λ CDM cosmology. From this Union 2.1 compilation, the χ^2 value is computed

$$\chi_{\text{Sn}}^2 = \sum_{i=1}^{N_{\text{Sn}}} \frac{(\mu_i^{\text{obs}} - \mu_i^{\text{th}}(z_i) - \Delta M)^2}{\sigma_{i,\text{Sn}}^2} + \frac{\Delta M^2}{(0.15^{\text{mag}})^2} \quad , \quad (11)$$

where the theoretical distance modulus $\mu_i^{\text{th}}(z_i)$ is computed from the luminosity distance $d_L(z)$ of the considered model. The parameter ΔM allows a small variation of the absolute magnitude $M_B \simeq -19.3^{\text{mag}}$ ($h = 0.7$) [39] of the supernovae Ia. The parameter ΔM is analytically marginalised [40]. The order of the variation 0.15^{mag} is estimated according [39]. When the supernovae data are used without other data sets, we constrain the variation of ΔM with the last summand in (11) because of the degeneracy between the Hubble constant h and the absolute magnitude M_B . A change in the absolute magnitude from M_B to M'_B corresponds to a shift of the Hubble constant h to h' with

$$M_B - M'_B = 5 \log_{10} \left(\frac{h'}{h} \right) \quad . \quad (12)$$

The difference of the measurement of the Hubble constant of [41] with a best estimate of $H_0 = 73.24 \pm 1.74$ km/(s Mpc) with the Planck value of $H_0 = 67.8 \pm 0.9$ km/(s Mpc) [42] corresponds to a shift of the absolute magnitude of $\Delta M \simeq 0.25^{\text{mag}}$. When we generate Markov chains Monte Carlo together with other data sets, we omit the last summand in (11) and left ΔM unconstrained in the marginalisation.

3.2. The BAO data

While the supernovae data constrain primarily the luminosity distance $d_L(z)$, the measurement of baryon acoustic oscillations allows the determination of the angular diameter distance $d_A(z)$ as well as the value of the Hubble length $d_H(z) := c/H(z)$. The standard ruler for these lengths is provided by the sound horizon

$$r_s = \int_{z_{\text{drag}}}^{\infty} \frac{c_s(z)}{H(z)} dz \quad (13)$$

at the drag epoch at redshift z_{drag} when photons and baryons decouple. The speed of sound $c_s(z)$ in the photon-baryon fluid is given by

$$c_s(z) = \frac{c}{\sqrt{3(1 + \mathcal{R}(z))}} \quad \text{with} \quad \mathcal{R}(z) = \frac{3\rho_{\text{bar}}}{4\rho_{\gamma}} = \frac{3}{4} \frac{\Omega_{\text{bar}}}{\Omega_{\gamma}} \frac{1}{z+1} \quad . \quad (14)$$

The drag redshift z_{drag} can be determined by using fitting formulae [43, 44] but since we are dealing with cosmological models that possibly leave the validity domain of the parameter space where these fitting formulae are valid, we use the exact approach. A drag depth is defined as [45]

$$\tau_{\text{drag}}(z) := \int_{\eta(z)}^{\eta_0} \frac{\dot{\tau}}{\mathcal{R}} d\eta \quad , \quad (15)$$

where τ is the Compton optical depth with $\dot{\tau}$ denoting its derivative with respect to conformal time η and $d\eta = c dt/a(t)$. The drag epoch is then determined by the redshift z_{drag} satisfying [45]

$$\tau_{\text{drag}}(z_{\text{drag}}) = 1 \quad . \quad (16)$$

With z_{drag} computed in this way, the equation (13) gives the standard ruler r_s which in turn allows the conversion of the BAO data such that a χ^2 analysis of the Chaplygin gas cosmology is possible.

In table 1 the BAO data used in this paper are listed. For redshifts $z < 0.2$ the data of the 6dF galaxy survey [46] and the SDSS Data Release 7 main galaxy sample [47] are used which are given in terms of volume averaged distances

$$d_V(z) := \sqrt[3]{z(1+z)^2 d_H(z) d_A^2(z)} \quad .$$

For $0.2 < z < 1$, the Data Release 12 of the SDSS-III/BOSS spectroscopic galaxy sample [48] is used, which are also given in table 1. The data for $H(z)$ and $d_A(z)$ are used simultaneously. Furthermore, the BAO data extracted from the auto-correlation of the Lyman α forest fluctuations of the BOSS Data Release 11 quasars [49] are used. In addition, the BAO data obtained from the quasar-Lyman α cross-correlation of the Data Release 11 of the SDSS-III/BOSS [50] are taken into account. Although both Lyman α data sets are derived from the same volume, they can be considered as independent data points as stated in [44]. The auto-correlation and cross-correlation approaches are complementary because of the quite different impact of redshift-space distortion on the two measurements. These BAO data can be considered as independent because their uncertainties are not dominated by cosmic variance, but instead are dominated by the combination of noise in the spectra and sparse sampling of the structure in the survey volume, both of which affect the auto-correlation and cross-correlation almost independently [44]. In order to substantiate this, tests with mock catalogues and several analysis procedures are carried out in [49], which find a good agreement between error estimates from the likelihood function and from the variance in mock catalogues. Thus, in our χ^2 analysis the $d_A(z)$ and $d_H(z)$ values of both Lyman α data sets are taken into account. It is worthwhile to note that the BAO data are biased towards the Λ CDM model especially for larger values of the redshift z , because of the necessary distance calibrations. Thus, the BAO data possess a model-dependence in favour of the concordance model.

The χ^2 values are computed in the usual way as

$$\chi_{\text{BAO}}^2 = \sum_{i=1}^{N_{\text{BAO}}} \frac{(X_i^{\text{obs}} - X_i^{\text{th}}(z_i))^2}{\sigma_{i,\text{BAO}}^2}, \quad (17)$$

where X_i stands for one of the corresponding distances listed in table 1.

redshift z	$H(z)r_s$	$d_A(z)/r_s$	$d_V(z)/r_s$	$d_H(z)/r_s$	Reference
0.106			3.06 ± 0.13		6dFGS [46]
0.15			4.47 ± 0.17		SDSS DR7 [47]
0.24	11636.0 ± 827	5.59 ± 0.30			SDSS-III/BOSS DR12 [48]
0.32	11075.0 ± 591	6.47 ± 0.19			
0.37	11045.0 ± 930	6.72 ± 0.44			
0.49	12920.0 ± 709	8.72 ± 0.21			
0.59	14279.0 ± 399	9.62 ± 0.16			
0.64	14530.0 ± 546	9.78 ± 0.28			
2.34		11.28 ± 0.65		9.18 ± 0.28	DR11 Ly α (auto) [49]
2.36		10.8 ± 0.4		9.00 ± 0.30	DR11 Ly α (cross) [50]

Table 1: The BAO data used for constraining the generalised Chaplygin gas cosmology.

3.2.1. On the significance of the Lyman α data

The addition of the Lyman α data to the χ^2 analysis significantly constrains the models of the Chaplygin cosmology due to their larger redshift. In order to show this, the figures 1 and 2 show the 1σ and 2σ confidence domains for several Chaplygin cosmologies with a fixed value of α as defined in equation (1) using the BAO data of table 1 with and without the Lyman α data. The figures do not show the confidence domains with respect to the parameters that are varied in the MCMC algorithm, but instead, they show the combinations $\Omega_{\text{Chap}} - \Omega_{\text{Chap}}^{\text{eff}}$ and $\Omega_{\text{bar}} + \Omega_{\text{Chap}}^{\text{eff}}$ where $\Omega_{\text{Chap}}^{\text{eff}}$ is defined in (7). For the special case $\alpha = 0$ corresponding to the Λ CDM cosmology, the combination $\Omega_{\text{Chap}} - \Omega_{\text{Chap}}^{\text{eff}}$ corresponds to the contribution of the cosmological constant Ω_{Λ} and $\Omega_{\text{bar}} + \Omega_{\text{Chap}}^{\text{eff}}$ to the matter content Ω_{mat} as outlined in section 2.

The figure 1(a) shows the confidence domains without the constraining power of the Lyman α data, that is using the values of table 1 with $z < 1$, for four Chaplygin cosmologies with $\alpha = 0, \frac{1}{3}, \frac{2}{3},$ and 1. The figure reveals very large confidence domains. The cut-off like behaviour of the confidence domains around $\Omega_{\text{bar}} + \Omega_{\text{Chap}}^{\text{eff}} \simeq 0.16$ is due to the restriction $B < 1$ which avoids phantom-like energy at the current epoch and a singular behaviour of the equation of state in the past (see section 2).

Including the Lyman α data reduces drastically the confidence domains so that the restriction to $B < 1$ does not become appreciable as shown in figure 1(b). It is seen that with increasing values of α , the best-fit region prefers lower densities of Ω_{tot} . While the Chaplygin cosmology with $\alpha = 0$ prefers models with a positive spatial curvature ($\Omega_{\text{tot}} > 1$), the revers is true for the case $\alpha = 1$.

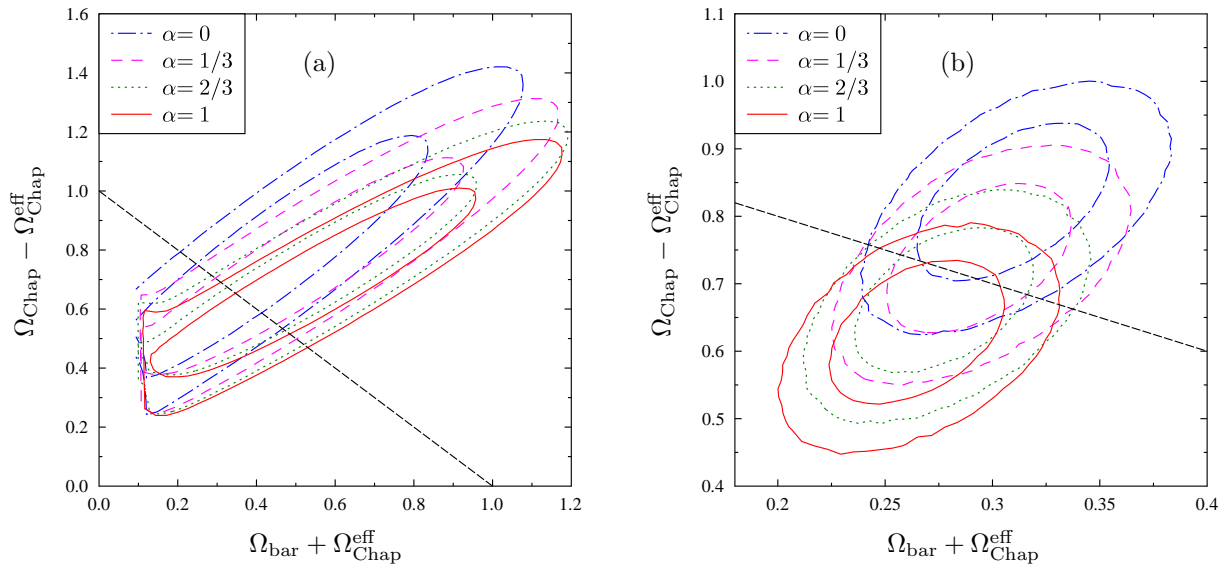


Figure 1: The 1σ and 2σ confidence contours are shown with respect to effective matter and energy density for four Chaplygin models with fixed values of α . The panel (a) uses the BAO data without the Ly α values, whereas the panel (b) includes them. Note the different scales on the axes. The dashed line corresponds to universes with $\Omega_{\text{tot}} = 1$.

The figure 2(a) displays the 1σ and 2σ confidence domains for $\alpha = 0$ and for $\alpha = 1$ with and without the Lyman α data in one plot and emphasises the restrictions due to them.

Recently, the SDSS DR12 data have been used to compute the auto-correlation of the Lyman α forest fluctuations and to derive updated values of $d_A(z)$ and $d_H(z)$ for $z = 2.33$ [51]. The updated distances $d_A(z = 2.33)/r_s = 11.34 \pm 0.64$ and $d_H(z = 2.33)/r_s = 9.07 \pm 0.31$ agree with the previous Lyman α results derived from the Data Release 11 [49, 50] within $\sim 0.5\sigma$ [51]. In order to compare these updated auto-correlation based new data, two Monte Carlo chains are generated, where one chain uses the BAO data as listed in table 1 with the Lyman α derived values of DR11. In the other chain, the auto-correlation derived DR11 values of [49] are replaced by the updated DR12 values of [51]. The result is shown in figure 2(b). The confidence regions are shifted relative to each other, but there is nevertheless a large overlap between them. This demonstrates the sensitivity due to the data point around $z = 2.34$. However, as it is also the case for the supernovae data, the BAO data and especially the Lyman α forest data are also contaminated by the Λ CDM model which enters in the distance calibration.

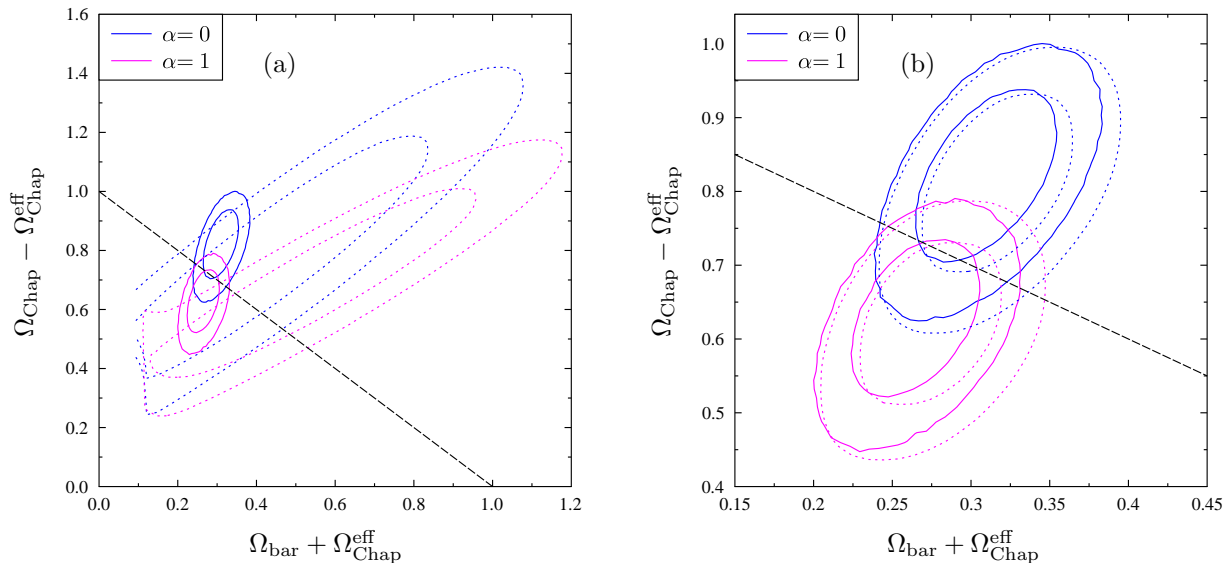


Figure 2: To emphasise the restricting power of the Ly α data around $z = 2.34$, the 1σ and 2σ confidence contours are shown with respect to effective matter and effective dark energy density for two Chaplygin models with $\alpha = 0$ and $\alpha = 1$. The dotted curves in panel (a) are computed using only the BAO data below $z = 1$ as in figure 1(a), while the full curves take also the Lyman α forest derived data of table 1 into account. The panel (b) shows the shift of the confidence domains when the auto-correlation derived Lyman α DR11 data (full curves) are replaced with those of DR12 (dotted curves) while leaving the other BAO data unchanged. The dashed line indicates the positions of the models with $\Omega_{\text{tot}} = 1$ in both panels.

3.3. The cosmic microwave background data of Planck 2015

The supernovae Ia and BAO data discussed above provide likelihood estimations for cosmological models with respect to their background behaviour. The angular power spectrum $\mathcal{D}_l^{\text{TT}} := l(l+1)C_l^{\text{TT}}/(2\pi)$ of the cosmic microwave background radiation, on the other hand, tests the evolution of perturbations. The multipole spectrum C_l^{TT} is defined by

$$C_l^{\text{TT}} = \frac{1}{2l+1} \sum_{m=-l}^l |a_{lm}|^2$$

where a_{lm} are the expansion coefficients of the temperature fluctuations with respect to the spherical harmonics. In this paper, the $\mathcal{D}_l^{\text{TT}}$ measurements of the Planck 2015 data release [42] are used. The likelihood for a theoretical angular power spectrum $\mathcal{D}_l^{\text{TT}}$ is calculated with the Planck Likelihood Code R2.00 provided on the Planck website <http://pla.esac.esa.int/pla/#cosmology> which computes the log likelihoods of the temperature maps. These log likelihoods are then converted to the corresponding χ_{CMB}^2 to be used in (10). The low- l likelihood based on the results of the Commander approach is calculated for $l = 2$ to 29 using the file `commander_rc2_v1.1_12_29_B.clik` which is also given at the Planck website. Since the $\mathcal{D}_l^{\text{TT}}$ spectra for the Chaplygin gas cosmology are computed up to $l = 1000$, we use for the high- l likelihood the file `plik_dx11dr2_HM_v18_TT.clik` ($29 < l < 2509$) modified to cover the multipole range $29 < l \leq 1000$. The restriction to the multipole range $l \leq 1000$ reduces significantly the CPU time of the MCMC estimations.

The $\mathcal{D}_l^{\text{TT}}$ spectra for the Chaplygin gas cosmology are computed with the code described in [36]. In this code, the isentropic initial conditions are specified at conformal time $\eta = 0$. Then, power series in η for the various perturbations are used to analytically compute the perturbations at $\eta = \eta_{\text{rec}}/200$, where η_{rec} denotes the time of recombination. With these values, the Boltzmann equations are integrated numerically up to the present epoch leading to the theoretical $\mathcal{D}_l^{\text{TT}}$ spectra. The perturbation power series, which are derived in [36], allow a faithful treatment of the initial conditions towards a later time, since for $\eta \rightarrow 0$, a numerical integration of the system of differential equations is not possible due to the singular behaviour of various terms at $\eta = 0$. This singular behaviour leads to a cancellation of numerical digits by the subtraction of very large terms of the same magnitude. This difficulty is circumvented by using analytic power series in the interval $\eta \in [0, \eta_{\text{rec}}/200]$. Since there are no such accuracy problems for $\eta > \eta_{\text{rec}}/200$, the integration of the perturbation equations can then be done numerically for these large values of η . The validity of our code is checked by comparing the $\mathcal{D}_l^{\text{TT}}$ spectra for the Λ CDM model for a wide range of curvatures obtained from our code with those computed with the public software CAMB¹.

Besides the equation of state, there are further degrees of freedom which characterise the Chaplygin gas, or a general dark matter component, as em-

¹The software is available at <http://camb.info>

phasised by Hu [14], where a generalised dark matter component is introduced which is defined by the effective velocity of sound c_{eff} (in the rest frame of the dark component) and a viscosity velocity c_{vis} which is related to the anisotropic stress. The effective speed of sound can be interpreted as the rest frame speed of sound

$$c_{\text{eff}}^2 = \frac{\delta p_g^{(\text{rest})}}{\delta \rho_g^{(\text{rest})}} \quad , \quad (18)$$

where the pressure and density perturbations in the rest frame of the generalised dark matter component are denoted by $\delta p_g^{(\text{rest})}$ and $\delta \rho_g^{(\text{rest})}$. In this paper, both velocities are set to zero $c_{\text{eff}}^2 = c_{\text{vis}}^2 = 0$. For a UDM model, $\mathcal{D}_l^{\text{TT}}$ spectra for a positive c_{eff}^2 are shown in figures 7 and 8 in [36].

The theoretical $\mathcal{D}_l^{\text{TT}}$ spectra depend on the scalar spectral index n_s and the overall normalisation. After computing the CMB transfer function for a model of the MCMC sequence, these two quantities are determined such that the value of χ_{CMB}^2 computed by the Planck Likelihood Code is minimised. Thus, neither n_s nor the overall normalisation occur as free parameters in the MCMC sequence. Furthermore, the reionisation is modelled by a smooth transition with a width $\Delta z = 0.4$ at a redshift $z_{\text{reion}} = 10.6$, at which half of the matter is reionised. The choice of z_{reion} and Δz does not sensitively influence the likelihood, see e.g. figure 6 in [36], where $\mathcal{D}_l^{\text{TT}}$ is computed for two different values of the reionisation optical depth. The $\mathcal{D}_l^{\text{TT}}$ spectra are only changed at small values of l , where the data possess large uncertainties.

4. Analysis and Results

4.1. MCMC analysis for a fixed value of α

In this subsection, the best-fit estimates are considered for fixed values of the equation of state parameter α . The aim is to reveal which data set is responsible for the shift of the best-fit parameters. On the one hand, MCMC sequences are generated which take into account only one of the data sets BAO, SN and CMB as discussed above. Their χ^2 values are denoted as χ_{BAO}^2 , χ_{SN}^2 and χ_{CMB}^2 and the best-fit models minimise only one of the three χ^2 values and ignore the other two. On the other hand, further MCMC sequences are generated that take all three data sets simultaneously into account whose χ^2 value is the corresponding sum

$$\chi_{\text{BAO+SN+CMB}}^2 = \chi_{\text{BAO}}^2 + \chi_{\text{SN}}^2 + \chi_{\text{CMB}}^2 \quad (19)$$

and their best-fit model minimises $\chi_{\text{BAO+SN+CMB}}^2$. Thus, we consider four kinds of best-fit models which minimise χ_{BAO}^2 , χ_{SN}^2 , χ_{CMB}^2 , and $\chi_{\text{BAO+SN+CMB}}^2$, respectively. The individual components in (19) belonging to the smallest total value $\chi_{\text{BAO+SN+CMB}}^2$ are denoted as $\bar{\chi}_{\text{BAO}}^2$, $\bar{\chi}_{\text{SN}}^2$, and $\bar{\chi}_{\text{CMB}}^2$. These are, in general, larger than the smallest χ^2 values of the MCMC sequences which take only one data set into account. The difference between the smallest values of χ_{BAO}^2 , χ_{SN}^2 , and χ_{CMB}^2 with the corresponding values of $\bar{\chi}_{\text{BAO}}^2$, $\bar{\chi}_{\text{SN}}^2$, and $\bar{\chi}_{\text{CMB}}^2$ reveals the tension between the three data sets with respect to a cosmological

model. This difference indicates how far the optimal cosmological parameters with respect to a single data set are driven away in order to yield the best compromise with respect to all three data sets. In the case of a perfect concordance between the three data sets, one would obtain $\chi_{\text{BAO}}^2 = \bar{\chi}_{\text{BAO}}^2$, $\chi_{\text{SN}}^2 = \bar{\chi}_{\text{SN}}^2$, and $\chi_{\text{CMB}}^2 = \bar{\chi}_{\text{CMB}}^2$.

α	χ_{BAO}^2	$\bar{\chi}_{\text{BAO}}^2$	χ_{SN}^2	$\bar{\chi}_{\text{SN}}^2$	χ_{CMB}^2	$\bar{\chi}_{\text{CMB}}^2$	$\chi_{\text{BAO+SN+CMB}}^2$
-2/3	11.94	96.49	562.34	764.92	1376.69	1389.37	2250.78
-1/3	12.30	33.35	562.26	602.37	1385.99	1392.28	2028.00
0	18.46	21.33	562.23	563.05	1390.91	1393.43	1977.80
1/3	25.81	26.61	562.20	571.21	1394.71	1395.67	1993.49
2/3	32.04	36.44	562.18	594.57	1397.13	1398.45	2029.45
1	36.74	47.26	562.16	620.07	1398.90	1400.95	2068.28

Table 2: The minimum of χ^2 is given for several fixed values of the equation of state parameter α . The columns with χ_{BAO}^2 , χ_{SN}^2 and χ_{CMB}^2 list the minimum of χ^2 , if only the corresponding data set is used. The column with $\chi_{\text{BAO+SN+CMB}}^2$ lists the minimum if all three data sets are used simultaneously, and $\bar{\chi}_{\text{BAO}}^2$, $\bar{\chi}_{\text{SN}}^2$, $\bar{\chi}_{\text{CMB}}^2$ are the individual components contributing to the minimal value of $\chi_{\text{BAO+SN+CMB}}^2$.

α	χ_{BAO}^2	$\bar{\chi}_{\text{BAO}}^2$	χ_{SN}^2	$\bar{\chi}_{\text{SN}}^2$	χ_{CMB}^2	$\bar{\chi}_{\text{CMB}}^2$	$\chi_{\text{BAO+SN+CMB}}^2$
0	9.62	10.52	562.23	563.03	1390.91	1393.28	1966.83
1/3	9.17	15.48	562.20	569.52	1394.71	1396.23	1981.23
2/3	8.84	23.79	562.18	591.77	1397.13	1399.11	2014.67
1	8.66	31.11	562.16	618.36	1398.90	1401.74	2051.20

Table 3: In contrast to table 2, we use here only the BAO data without those derived from the Lyman α forest, that is without the BAO values at $z \simeq 2.34$. All other data sets are the same as used in table 2.

In table 2 the minimal values of χ^2 are given for the generalised Chaplygin gas model for several fixed values of the parameter α as defined in (1). The table reveals that the supernovae data in isolation are the least stringent ones since they always give χ_{SN}^2 values around 562.2 independently of α . At second comes the CMB data, whose χ_{CMB}^2 values increases by 8 from $\alpha = 0$ to $\alpha = 1$. In contrast, the BAO data lead for the same range of α to the largest increase by 18.3. Concerning the values of α given in table 2, one concludes that the data sets prefer the value $\alpha = 0$ which corresponds to the Λ CDM model. It is interesting to note that the CMB data alone possesses even smaller values of χ_{CMB}^2 for negative values of α as revealed by table 2.

As the subsection 3.2.1 has shown, the most stringent power of the BAO data stems from the inclusion of the Lyman α forest derived BAO data around the redshift $z \simeq 2.34$. The Lyman α forest data consists of four data points which belong to $d_A(z)/r_s$ and $d_H(z)/r_s$ obtained from the cross- and the auto-correlation approach each given in table 1. Omitting these data around $z \simeq 2.34$ reduces the power of the BAO data set. To demonstrate that, the table 3

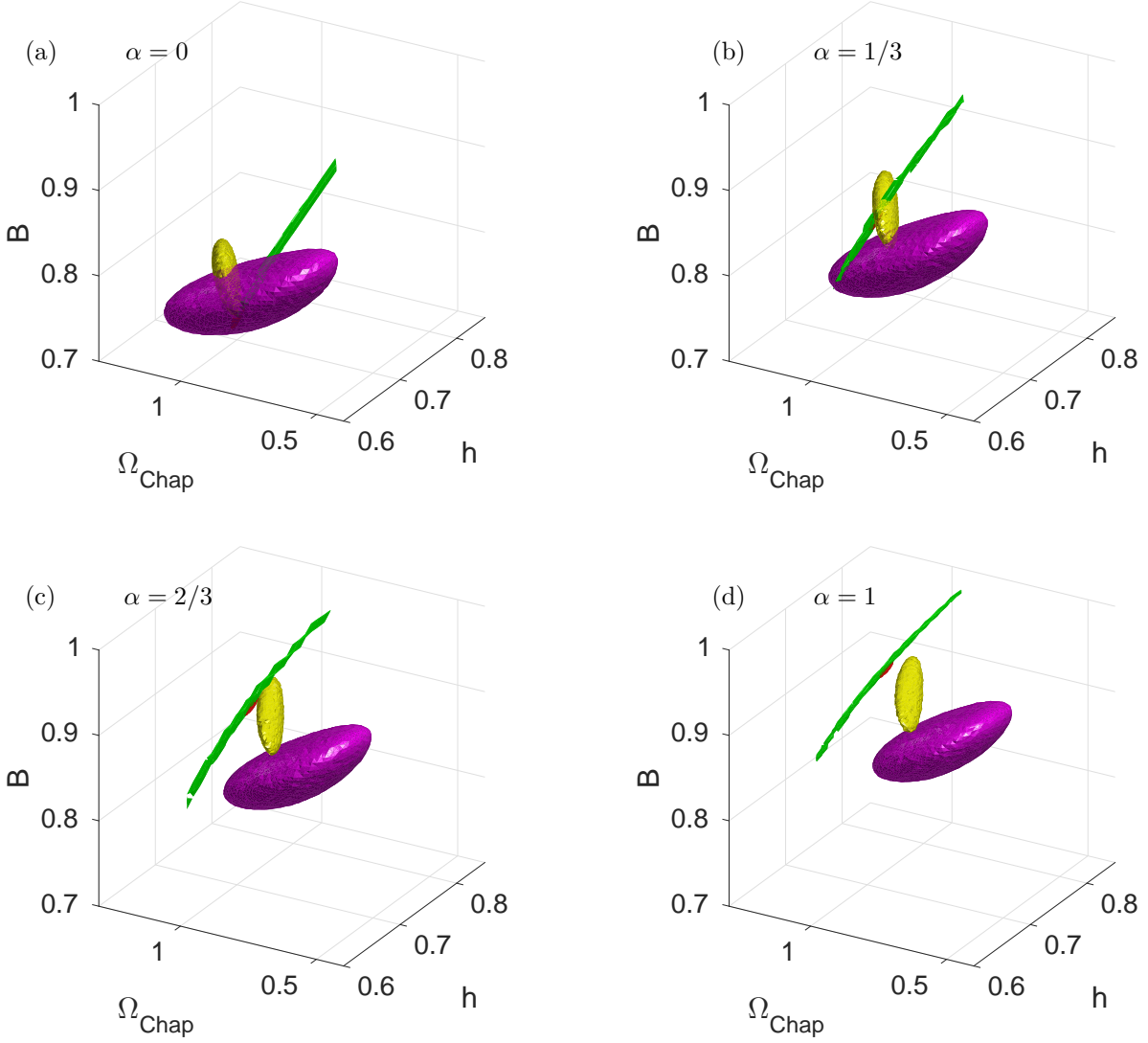


Figure 3: The concordance between the three cosmological data sets is presented. The 1σ confidence domains are shown for the four Chaplygin gas models with fixed parameter $\alpha = 0, 1/3, 2/3,$ and 1 . The axes denote the parameters that are varied in the MCMC sequences, that is $h, \Omega_{\text{Chap}},$ and B . The domain belonging to the supernovae data is shown in magenta, the BAO domain in yellow, the CMB domain in green, and the combined χ^2 search in red. The projections are the same in all panels.

shows the results obtained from MCMC sequences which use only the BAO data without the data around $z \simeq 2.34$, but the supernovae and CMB data are the same in the case of the joint analysis. While χ_{BAO}^2 takes on its minimum around $\alpha \simeq -0.52$ (not listed in table 2) by including the $z \simeq 2.34$ data, that minimum is shifted to $\alpha \simeq +1.4$ by omitting the high z data, although this minimum belongs to an unrealistically large value for the Hubble constant. Furthermore, as the comparison of the column for χ_{BAO}^2 of table 2 with that of table 3 shows, the dependence of χ_{BAO}^2 on α is rather weak without the $z \simeq 2.34$ data. Table 3 reveals the modest increase by one for χ_{BAO}^2 by changing $\alpha = 0$ to $\alpha = 1$, which has to be compared with the increase of 18.3 by using the Lyman α data. Let us now turn to the joint analysis, where the MCMC sequences take the BAO, supernovae, and CMB data simultaneously into account. Here the comparison of the columns $\bar{\chi}_{\text{BAO}}^2$ of tables 2 and 3 shows that the contribution $\bar{\chi}_{\text{BAO}}^2$ from the BAO data to the minimum $\chi_{\text{BAO+SN+CMB}}^2$ is reduced by more than ten without the $z \simeq 2.34$ data although only four data points are left out. This demonstrates the tension of the $z \simeq 2.34$ data with the Chaplygin gas cosmology. It was already found in [49] that the auto-correlation derived DR11 values of the Lyman α forest lead to values that deviate by 7% from the predictions of the Λ CDM model. Thus the tension is also present in the Λ CDM model, but the Chaplygin gas cosmology provides no remedy in this respect.

The value $\alpha = 0$ is preferred by the MCMC sequences which use the joint data sets $\chi_{\text{BAO+SN+CMB}}^2$ as seen in tables 2 and 3. Let us now turn to table 2, where the $z \simeq 2.34$ data are included. Here, the least difference $\bar{\chi}_{\text{BAO}}^2 - \chi_{\text{BAO}}^2$ for the BAO data occurs for $\alpha = 1/3$, while the smallest difference $\bar{\chi}_{\text{SN}}^2 - \chi_{\text{SN}}^2$ due to the supernovae data happens at $\alpha = 0$. The CMB data show only a modest increase by one for $\alpha = 1/3$ and $\alpha = 2/3$. So one concludes that although the total $\chi_{\text{BAO+SN+CMB}}^2$ value is minimal for $\alpha = 0$, the tension between the BAO and CMB data sets is reduced for α around $1/3$.

In order to visualise these dependencies, the figure 3 shows the 1σ confidence domains generated by the various MCMC sequences for the four fixed values $\alpha = 0, 1/3, 2/3, \text{ and } 1$. Here and in the following, the BAO data are used including the $z \simeq 2.34$ data. The 1σ confidence domains are chosen instead of, e.g. 2σ confidence domains, because of their reduced volume and, thus, they show more clearly the shifting in the parameter space. The domains belonging to the CMB chains (shown in green) extend to large values of the Hubble constant h and, for clarity, are truncated at $h = 0.85$ in figure 3. The domains belonging to the supernovae chains are shown in magenta and those of the BAO chains in yellow, while the confidence domains of the total MCMC chains are plotted in red.

For $\alpha = 0$ the red confidence domain of the total $\chi_{\text{BAO+SN+CMB}}^2$ MCMC sequences is within that of the supernovae close to the common intersection point of the three 1σ confidence domains each belonging to a single data set. This concordance between the data sets is removed with increasing α . For $\alpha = 1/3$ there is no common overlap between the three individual 1σ confidence domains, although each pair of them possesses one. This gets worse for $\alpha = 2/3$ as seen in figure 3(c), where the CMB and the supernovae domains do not

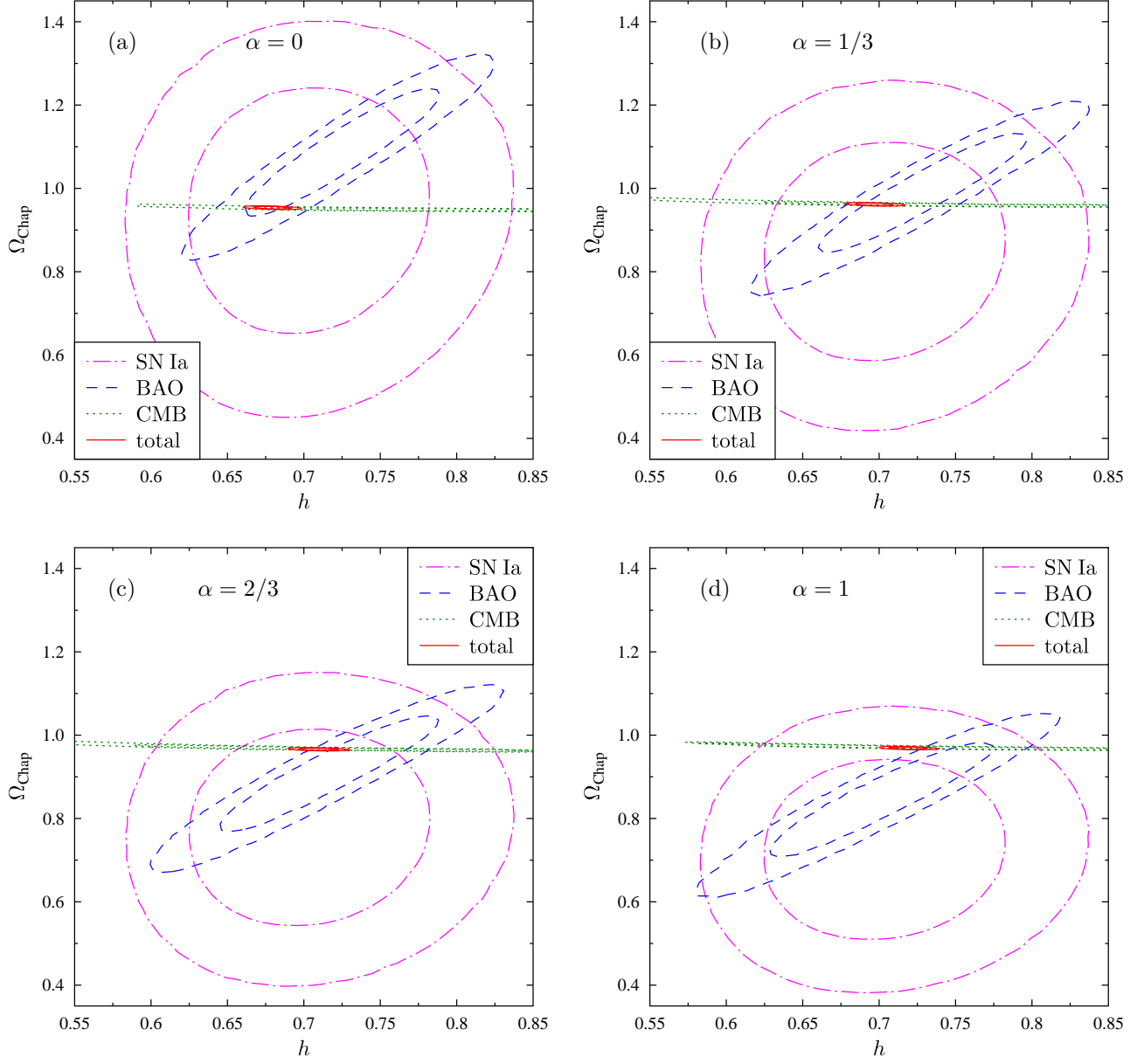


Figure 4: The 1σ and 2σ confidence contours are shown for the four Chaplygin gas models with fixed parameter $\alpha = 0, 1/3, 2/3,$ and 1 . The confidence domains are projected onto the $h - \Omega_{\text{Chap}}$ plane. To emphasise the shift of the confidence domains depending on α , all four panels use the same scaling at the axes.

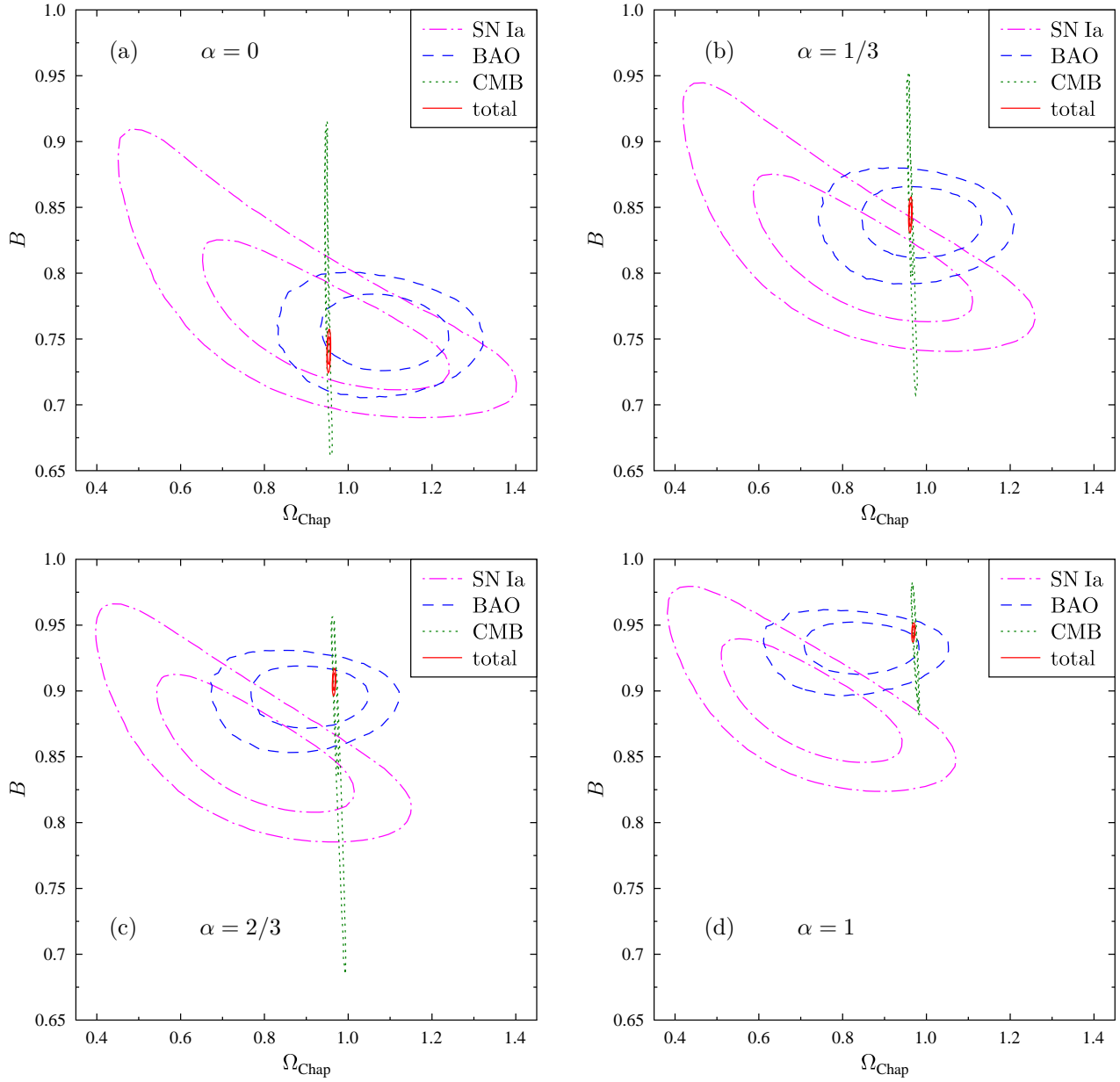


Figure 5: The 1σ and 2σ confidence contours are shown for the four Chaplygin gas models with fixed parameter $\alpha = 0, 1/3, 2/3,$ and 1 . The confidence domains are projected onto the $\Omega_{\text{Chap}} - B$ plane. As in figure 4, all four panels use the same scaling at the axes.

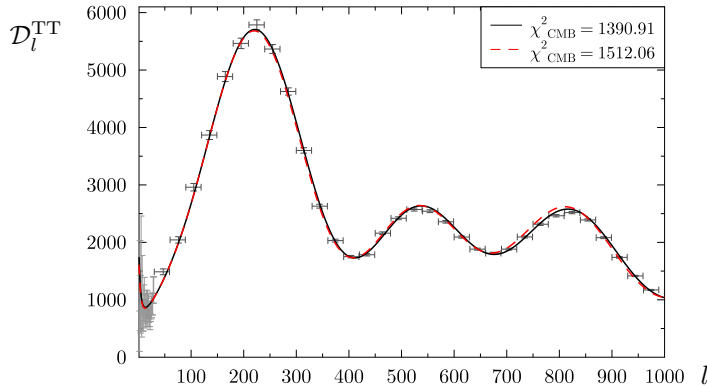


Figure 6: Two angular power spectra $\mathcal{D}_l^{\text{TT}}$ are shown for $\alpha = 0$, which possess different values of χ_{CMB}^2 . The full curve belongs to the model with the lowest value of χ_{CMB}^2 for the case $\alpha = 0$ ($h = 0.8859$, $\Omega_{\text{bar}} = 0.0284$, $\Omega_{\text{Chap}} = 0.9476$, $B = 0.8471$) while the dashed curve belongs to a model with a χ_{CMB}^2 value which is higher by 121 ($h = 0.8570$, $\Omega_{\text{bar}} = 0.0304$, $\Omega_{\text{Chap}} = 0.9488$, $B = 0.8309$). The binned data of the Planck 2015 data release [42] are plotted for $l > 30$ with the corresponding error bars, while up to $l = 29$ all data points are shown.

overlap at all and those of the supernovae and BAO are separated by a tiny gap. For $\alpha = 1$ the separation between the confidence domains increases further. It is worthwhile to note that the red confidence domain tends to be close to that of the CMB domain, which is a consequence of the constraining power of the Planck Likelihood Code. The inspection of the $\mathcal{D}_l^{\text{TT}}$ spectra for the Chaplygin gas cosmology reveals that a very steep increase of the χ_{CMB}^2 values occurs due to a slight mismatch of the second and third acoustic peak compared to those measured by Planck. In order to illustrate this sensitivity, figure 6 displays the angular power spectra $\mathcal{D}_l^{\text{TT}}$ of two models whose χ_{CMB}^2 values differ by 121. A difference in $\mathcal{D}_l^{\text{TT}}$ is only appreciable at the third acoustic peak.

In figures 4 and 5, the projections of the 1σ confidence domains of the three-dimensional plots of figure 3 are shown on a two parameter plane and, in addition, the 2σ confidence domains are also plotted. This perspective allows a more quantitative comparison of the confidence domains, especially how far they overlap. The figure 4 displays these domains in the $h - \Omega_{\text{Chap}}$ plane. As already noted in connection with figure 3, the confidence domains of the CMB data are very thin bands which are projected onto the horizontal bands in figure 4. Comparing the 1σ confidence domains belonging to the joint analysis of the four panels in figure 4, one observes that the Hubble constant h increases with α . This is a consequence of the BAO data as a comparison of the four panels in figure 4 reveals. The confidence domains belonging to the BAO data move to lower values of Ω_{Chap} with increasing α and due to their inclination within the $h - \Omega_{\text{Chap}}$ plane, the intersection with the CMB contours occurs at higher values of h . Figure 5, where the $\Omega_{\text{Chap}} - B$ plane is plotted, shows that B

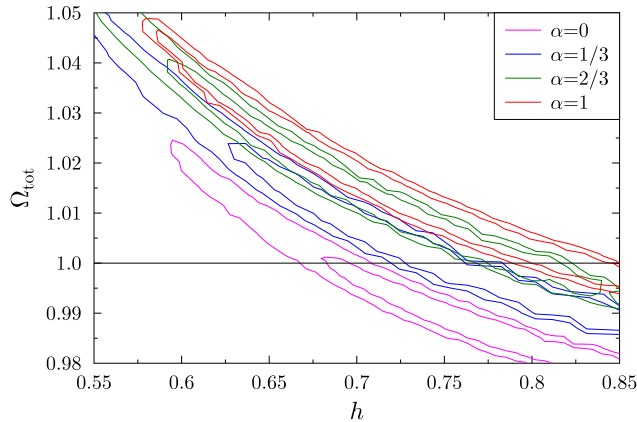


Figure 7: The 1σ and 2σ confidence contours computed from the CMB data are shown projected onto the $h - \Omega_{\text{tot}}$ plane. The confidence contours belong to the four Chaplygin gas models with a fixed parameter $\alpha = 0, 1/3, 2/3,$ and 1 . The horizontal line indicates spatially flat models with $\Omega_{\text{tot}} = 1$.

also increases with α . This behaviour stems again from the BAO data, since the CMB data lead to the vertical bands in figure 5 allowing a wide range of values of B . Because of $w_{\text{Chap}}(z = 0) = -B$, the current equation of state (3) tends towards more negative values. If the values of $w_{\text{Chap}}(z = 0)$ are to be compared with the Λ CDM model, one has to combine the equation of state of the CDM component with that of the cosmological constant leading to $w_{\Lambda\text{CDM}}(z = 0) = -1/(1 + \Omega_{\text{CDM}}/\Omega_{\Lambda})$.

The CMB data point to more or less spatially flat models since Ω_{tot} , equation (8), turns out to be of order one. Figure 7 shows that the confidence domains projected onto the $h - \Omega_{\text{tot}}$ plane shift to larger values of Ω_{tot} with increasing α , which is the reverse behaviour as it is observed in the case of the BAO data. But the shift caused by the CMB data is so small that the confidence domains overlap for neighbouring values of α . Note also, that only the small interval $[0.98, 1.05]$ for Ω_{tot} is displayed. Furthermore, the figure demonstrates that a possible restriction to spatially flat models in the MCMC sequences leads to larger values of the Hubble constant h with increasing α . Without such a restriction, the confidence domains for $\alpha = 0$ point to a slightly negative curvature, while for $\alpha = 2/3$ and $\alpha = 1$ a positive curvature is preferred, unless unrealistically large values of h are accepted.

4.2. MCMC analysis with varying values of α

In the previous subsection 4.1, the results are presented for MCMC sequences in which the equation of state parameter α is held fixed. This choice is motivated by the fact that $\alpha = 1$ corresponds to the originally proposed Chaplygin gas cosmology, while $\alpha = 0$ leads to the background cosmology of the Λ CDM model. So these two α values and two intermediate values are chosen for the analysis which shows that $\alpha = 0$ is superior compared to the other three values of α if

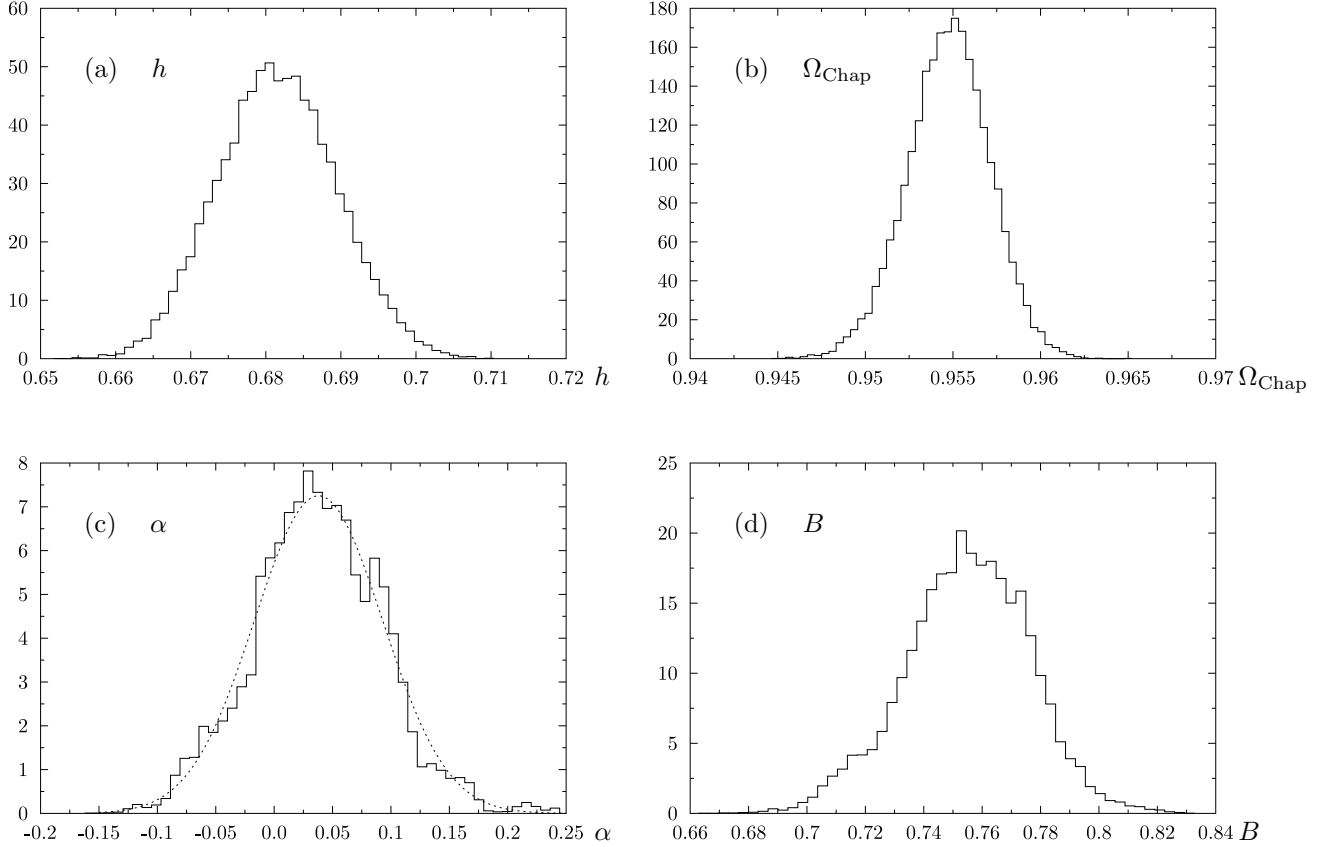


Figure 8: The distribution of the parameters derived from the MCMC sequence with varying values of α . In panel (c) the distribution of the α parameter is compared to a normal distribution with mean $\bar{\alpha} = 0.038$ and width 0.055. The value $\alpha = 0$ is thus within the 1σ confidence interval, but the best-fit models are close to $\alpha = 0.04$.

all three data sets are simultaneously taken into account. Since the differences in these α values are relatively large, a further MCMC sequence is generated with 150000 iterations, which varies also the parameter α in addition to the previously varied parameters h , Ω_{Chap} , and B . The parameter α is restricted to $\alpha > -1$ in the MCMC sequence. In that way, the distribution of the α values can be inferred. In this section, the analysis takes all BAO data given in table 1 as well as the above supernovae and CMB data into account. The best-fit Chaplygin model obtained in this MCMC sequence has $\chi^2_{\text{BAO+SN+CMB}} = 1977.53$, which is only marginally smaller than the value in table 2 for $\alpha = 0$.

The obtained distributions for the four parameters are shown in figure 8. The mean values and their 1σ deviations are $h = 0.6816 \pm 0.0079$, $\Omega_{\text{Chap}} = 0.9547 \pm 0.0024$, $\alpha = 0.038 \pm 0.055$, and $B = 0.755 \pm 0.021$. The obtained value

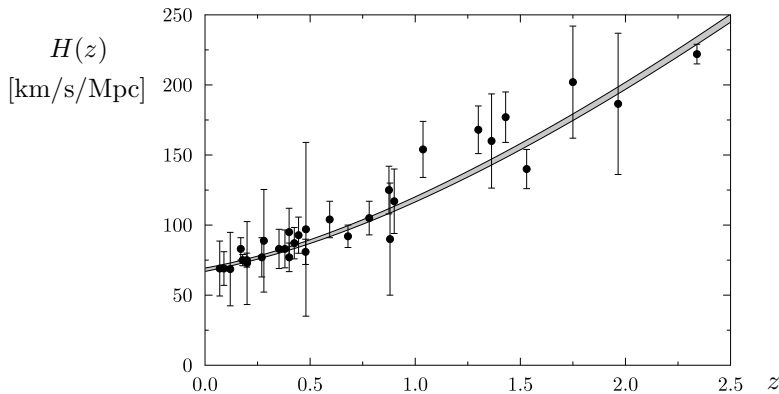


Figure 9: The variation of the Hubble parameter $H(z)$ is shown as a grey band for those Chaplygin gas cosmologies which are within the 1σ confidence domain with respect to $\chi^2_{\text{BAO+SN+CMB}}$. The observational Hubble data are taken from the compilation [52]. The Lyman α forest derived Hubble parameter at $z = 2.34$ is also plotted.

of the Hubble constant h is in agreement with the low value found by Planck [42]. It is worthwhile to note that this does not arise from the supernovae data since the last term in (11) is omitted in this joint analysis, and thus, there is no prior in h . As stated below (11) this term is only taken into account when the supernovae data are used alone. The Λ CDM model, which corresponds to $\alpha = 0$, is within the 1σ confidence interval although the peak of the distribution is shifted to larger values of α . The value of Ω_{Chap} is also in the range expected from the Λ CDM model. Assuming $\Omega_{\text{CDM}} \simeq 0.25$ and $\Omega_{\Lambda} \simeq 0.7$, the dark component contribution of the Λ CDM model is of the order 0.95 which agrees with Ω_{Chap} . The dark components of the Λ CDM model lead to the effective equation of state $w_{\Lambda\text{CDM}}(z = 0) = -1/(1 + \Omega_{\text{CDM}}/\Omega_{\Lambda})$ which is thus of the order $w_{\Lambda\text{CDM}}(z = 0) \simeq -0.74$ which in turn lies within the corresponding 1σ confidence interval for $w_{\text{Chap}}(z = 0) = -B$. The total density is obtained as $\Omega_{\text{tot}} = 1.0028 \pm 0.0026$ which thus shows a tendency towards positive curvature.

Figure 9 shows the variation of the Hubble parameter $H(z)$ for redshifts below $z = 2.5$. The distribution shown as a grey band is computed from all Chaplygin gas cosmologies which are within the 1σ confidence domain according to the joint analysis. Again, the MCMC models of the sequence with a varying parameter α are used. The figure also shows the observational Hubble data, which are taken from the compilation of [52]. In addition, the Hubble parameter at $z = 2.34$ derived from the Lyman α data is plotted [49]. The Chaplygin gas values match very well to the observations and their variation is much smaller than the 1σ errors of the data.

5. Summary

This paper discusses whether a better description of recent cosmological observations can be achieved, when the dark sector of the Λ CDM concordance model is replaced by the generalised Chaplygin gas. This prototypical model for a unified dark matter model with the equation of state $p = -A/\varepsilon^\alpha$ has the advantage that the Λ CDM model is recovered for $\alpha = 0$ at the background level. It turns out that the CMB statistics is the same for the generalised Chaplygin gas with $\alpha = 0$ and the Λ CDM cosmology in linear perturbation theory. This allows to test whether there are models in the neighbourhood of the concordance model that provide a better match to the data.

In this paper, the Planck 2015 cosmic microwave data, the SN Ia Union 2.1 compilation of the Supernova Cosmology Project, and the BAO data of the Data Release 12 of the SDSS-III/BOSS spectroscopic galaxy survey are used for a joint analysis with respect to the Chaplygin gas cosmology. Special emphasis is put on the four models with $\alpha = 0, 1/3, 2/3,$ and 1 . As visualised in figure 3, a concordance between the three sets of cosmological data is only obtained for values of α close to zero, where all three 1σ confidence domains overlap. Already for $\alpha = 1/3$ this concordance is lost and, at least at the 1σ level, there is no common overlap between the three confidence domains. The contribution of the BAO data to this behaviour depends on the inclusion of the Lyman α forest derived BAO data, as the comparison of table 2 with table 3 reveals. The strong increase of the χ^2 values of the BAO data is observed only by taking the Lyman α data into account. However, a more modest increase of χ^2 with increasing values of α is also observed for the CMB data, while the supernovae data show no dependence on α .

So the final conclusion is that the recent cosmological data favour values of α very close to zero. A joint analysis with varying values of α leads to $\alpha = 0.038 \pm 0.055$, which includes the Λ CDM model within the 1σ interval.

Acknowledgements

The Planck 2015 data [42] obtained from the LAMBDA website (<http://lambda.gsfc.nasa.gov>), the SN Ia Union 2.1 compilation of the Supernova Cosmology Project [39], and the SDSS-III/BOSS spectroscopic galaxy survey DR12 [48] are used in this work. The Planck Likelihood Code R2.00 provided on the Planck website <http://pla.esac.esa.int/pla/#cosmology> is also used.

References

References

- [1] D. Huterer, D. L. Shafer, Dark energy two decades after: Observables, probes, consistency tests, ArXiv e-prints [arXiv:1709.01091](https://arxiv.org/abs/1709.01091).

- [2] T. Buchert, A. A. Coley, H. Kleinert, B. F. Roukema, D. L. Wiltshire, Observational challenges for the standard FLRW model, *Int. J. Mod. Phys. D* 25 (2016) 1630007. [arXiv:1512.03313](#).
- [3] A. Kamenshchik, U. Moschella, V. Pasquier, An alternative to quintessence, *Physics Letters B* 511 (2001) 265–268. [arXiv:gr-qc/0103004](#).
- [4] J. C. Fabris, S. V. B. Goncalves, P. E. de Souza, Density perturbations in an Universe dominated by the Chaplygin gas, *Gen. Rel. Grav.* 34 (2002) 53–63. [arXiv:gr-qc/0103083](#).
- [5] N. Bilić, G. B. Tupper, R. D. Viollier, Unification of dark matter and dark energy: the inhomogeneous Chaplygin gas, *Physics Letters B* 535 (2002) 17–21. [arXiv:astro-ph/0111325](#).
- [6] M. C. Bento, O. Bertolami, A. A. Sen, Generalized Chaplygin gas, accelerated expansion, and dark-energy-matter unification, *Phys. Rev. D* 66 (2002) 043507. [arXiv:gr-qc/0202064](#).
- [7] M. C. Bento, O. Bertolami, A. A. Sen, Generalized Chaplygin gas and cosmic microwave background radiation constraints, *Phys. Rev. D* 67 (2003) 063003. [arXiv:astro-ph/0210468](#).
- [8] R. Bean, O. Doré, Are Chaplygin gases serious contenders for the dark energy?, *Phys. Rev. D* 68 (2003) 023515. [arXiv:astro-ph/0301308](#).
- [9] L. Amendola, F. Finelli, C. Burigana, D. Carturan, WMAP and the generalized Chaplygin gas, *J. Cosmology and Astroparticle Physics* 7 (2003) 005. [arXiv:astro-ph/0304325](#).
- [10] D. Carturan, F. Finelli, Cosmological effects of a class of fluid dark energy models, *Phys. Rev. D* 68 (2003) 103501. [arXiv:astro-ph/0211626](#).
- [11] M. Makler, S. Q. de Oliveira, I. Waga, Constraints on the generalized Chaplygin gas from supernovae observations, *Physics Letters B* 555 (2003) 1–6. [arXiv:astro-ph/0209486](#).
- [12] A. Dev, J. S. Alcaniz, D. Jain, Cosmological consequences of a Chaplygin gas dark energy, *Phys. Rev. D* 67 (2003) 023515. [arXiv:astro-ph/0209379](#).
- [13] H. B. Sandvik, M. Tegmark, M. Zaldarriaga, I. Waga, The end of unified dark matter?, *Phys. Rev. D* 69 (2004) 123524. [arXiv:astro-ph/0212114](#).
- [14] W. Hu, Structure formation with generalized dark matter, *Astrophys. J.* 506 (1998) 485–494. [arXiv:astro-ph/9801234](#).
- [15] R. R. Reis, I. Waga, M. O. Calvão, S. E. Jorás, Entropy perturbations in quartessence Chaplygin models, *Phys. Rev. D* 68 (2003) 061302. [arXiv:astro-ph/0306004](#).

- [16] K. Nozari, T. Azizi, N. Alipour, Observational constraints on Chaplygin cosmology in a braneworld scenario with induced gravity and curvature effect, *Mon. Not. R. Astron. Soc.* 412 (2011) 2125–2136. [arXiv:1011.3395](#).
- [17] R. Lamon, A. J. Wöhr, Quintessence and (anti-)Chaplygin gas in loop quantum cosmology, *Phys. Rev. D* 81 (2010) 024026. [arXiv:0910.4891](#).
- [18] X. Roy, T. Buchert, Chaplygin gas and effective description of inhomogeneous universe models in general relativity, *Class. Quantum Grav.* 27 (17) (2010) 175013. [arXiv:0909.4155](#).
- [19] M. C. Bento, O. Bertolami, M. J. Rebouças, P. T. Silva, Generalized Chaplygin gas model, supernovae, and cosmic topology, *Phys. Rev. D* 73 (2006) 043504. [arXiv:gr-qc/0512158](#).
- [20] P. Wu, H. Yu, Constraints on the unified dark energy dark matter model from latest observational data, *J. Cosmology and Astroparticle Physics* 3 (2007) 015. [arXiv:astro-ph/0701446](#).
- [21] L. Xu, J. Lu, Cosmological constraints on generalized Chaplygin gas model: Markov Chain Monte Carlo approach, *J. Cosmology and Astroparticle Physics* 3 (2010) 025. [arXiv:1004.3344](#).
- [22] J. P. Campos, J. C. Fabris, R. Perez, O. F. Piattella, H. Velten, Does Chaplygin gas have salvation?, *European Physical Journal C* 73 (2013) 2357. [arXiv:1212.4136](#).
- [23] Y.-Y. Xu, X. Zhang, Comparison of dark energy models after Planck 2015, *European Physical Journal C* 76 (2016) 588. [arXiv:1607.06262](#).
- [24] R. C. Freitas, S. V. B. Gonçalves, H. E. S. Velten, Constraints on the generalized Chaplygin gas model from Gamma-ray bursts, *Physics Letters B* 703 (2011) 209–216. [arXiv:1004.5585](#).
- [25] A. A. El-Zant, Unified dark matter: constraints from galaxies and clusters, *Mon. Not. R. Astron. Soc.* 453 (2015) 2250–2258. [arXiv:1507.07369](#).
- [26] J. Lu, L. Xu, Y. Wu, M. Liu, Combined constraints on modified Chaplygin gas model from cosmological observed data: Markov Chain Monte Carlo approach, *General Relativity and Gravitation* 43 (2011) 819–832. [arXiv:1105.1870](#).
- [27] B. C. Paul, P. Thakur, A. Beesham, Observational constraints on Modified Chaplygin Gas from Large Scale Structure, *ArXiv e-prints* [arXiv:1410.6588](#).
- [28] X. Zhang, F.-Q. Wu, J. Zhang, New generalized Chaplygin gas as a scheme for unification of dark energy and dark matter, *J. Cosmology and Astroparticle Physics* 1 (2006) 003. [arXiv:astro-ph/0411221](#).

- [29] B. Pourhassan, E. O. Kahya, FRW cosmology with the extended Chaplygin gas, *Adv. High Energy Phys.* 2014 (2014) 231452. [arXiv:1405.0667](#).
- [30] S. Carneiro, C. Pigozzo, Observational tests of non-adiabatic Chaplygin gas, *J. Cosmology and Astroparticle Physics* 10 (2014) 060. [arXiv:1407.7812](#).
- [31] R. F. vom Marttens, L. Casarini, W. Zimdahl, W. S. Hipólito-Ricardi, D. F. Mota, Does a generalized Chaplygin gas correctly describe the cosmological dark sector?, *Physics of the Dark Universe* 15 (2017) 114–124. [arXiv:1702.00651](#).
- [32] S. Wen, S. Wang, Comparing dark energy models with current observational data, *ArXiv e-prints* [arXiv:1708.03143](#).
- [33] J. R. Bond, G. Efstathiou, M. Tegmark, Forecasting cosmic parameter errors from microwave background anisotropy experiments, *Mon. Not. R. Astron. Soc.* 291 (1997) L33–L41. [arXiv:astro-ph/9702100](#).
- [34] G. Efstathiou, J. R. Bond, Cosmic confusion: degeneracies among cosmological parameters derived from measurements of microwave background anisotropies, *Mon. Not. R. Astron. Soc.* 304 (1999) 75–97. [arXiv:astro-ph/9807103](#).
- [35] M. Betoule, et al., Improved cosmological constraints from a joint analysis of the SDSS-II and SNLS supernova samples, *Astron. & Astrophys.* 568 (2014) A22. [arXiv:1401.4064](#).
- [36] R. Aurich, S. Lustig, Early-matter-like dark energy and the cosmic microwave background, *J. Cosmology and Astroparticle Physics* 1 (2016) 021. [arXiv:1511.01691](#).
- [37] M. Pettini, R. Cooke, A new, precise measurement of the primordial abundance of deuterium, *Mon. Not. R. Astron. Soc.* 425 (2012) 2477. [arXiv:1205.3785](#).
- [38] J. Dunkley, M. Bucher, P. G. Ferreira, K. Moodley, C. Skordis, Fast and reliable Markov chain Monte Carlo technique for cosmological parameter estimation, *Mon. Not. R. Astron. Soc.* 356 (2005) 925–936. [arXiv:astro-ph/0405462](#).
- [39] N. Suzuki, et. al, Supernova Cosmology Project, The Hubble Space Telescope Cluster Supernova Survey. V. Improving the Dark-energy Constraints above $z > 1$ and Building an Early-type-hosted Supernova Sample, *Astrophys. J.* 746 (2012) 85. [arXiv:1105.3470](#).
- [40] M. Goliath, R. Amanullah, P. Astier, A. Goobar, R. Pain, Supernovae and the nature of the dark energy, *Astron. & Astrophys.* 380 (2001) 6–18. [arXiv:astro-ph/0104009](#).

- [41] A. G. Riess, L. M. Macri, S. L. Hoffmann, D. Scolnic, S. Casertano, A. V. Filippenko, B. E. Tucker, M. J. Reid, D. O. Jones, J. M. Silverman, R. Chornock, P. Challis, W. Yuan, P. J. Brown, R. J. Foley, A 2.4% Determination of the Local Value of the Hubble Constant, *Astrophys. J.* 826 (2016) 56. [arXiv:1604.01424](#).
- [42] Planck Collaboration, R. Adam, P. A. R. Ade, N. Aghanim, Y. Akrami, M. I. R. Alves, M. Arnaud, F. Arroja, J. Aumont, C. Baccigalupi, et al., Planck 2015 results. I. Overview of products and scientific results, *Astron. & Astrophys.* 594 (2016) A1. [arXiv:1502.01582](#).
- [43] D. J. Eisenstein, W. Hu, Baryonic Features in the Matter Transfer Function, *Astrophys. J.* 496 (1998) 605–614. [arXiv:astro-ph/9709112](#).
- [44] É. Aubourg, et al., BOSS Collaboration, Cosmological implications of baryon acoustic oscillation measurements, *Phys. Rev. D* 92 (2015) 123516. [arXiv:1411.1074](#).
- [45] W. Hu, N. Sugiyama, Small-Scale Cosmological Perturbations: an Analytic Approach, *Astrophys. J.* 471 (1996) 542–570. [arXiv:astro-ph/9510117](#).
- [46] F. Beutler, C. Blake, M. Colless, D. H. Jones, L. Staveley-Smith, L. Campbell, Q. Parker, W. Saunders, F. Watson, The 6dF Galaxy Survey: baryon acoustic oscillations and the local Hubble constant, *Mon. Not. R. Astron. Soc.* 416 (2011) 3017–3032. [arXiv:1106.3366](#).
- [47] A. J. Ross, L. Samushia, C. Howlett, W. J. Percival, A. Burden, M. Manera, The clustering of the SDSS DR7 main Galaxy sample - I. A 4 per cent distance measure at $z = 0.15$, *Mon. Not. R. Astron. Soc.* 449 (2015) 835–847. [arXiv:1409.3242](#).
- [48] C.-H. Chuang, et. al, The Clustering of Galaxies in the Completed SDSS-III Baryon Oscillation Spectroscopic Survey: single-probe measurements from DR12 galaxy clustering – towards an accurate model, *Mon. Not. R. Astron. Soc.* 471 (2017) 2370–2390. [arXiv:1607.03151](#).
- [49] T. Delubac, et al., Baryon acoustic oscillations in the Ly α forest of BOSS DR11 quasars, *Astron. & Astrophys.* 574 (2015) A59. [arXiv:1404.1801](#).
- [50] A. Font-Ribera, et al., Quasar-Lyman α forest cross-correlation from BOSS DR11: Baryon Acoustic Oscillations, *J. Cosmology and Astroparticle Physics* 5 (2014) 027. [arXiv:1311.1767](#).
- [51] J. E. Bautista, et al., Measurement of BAO correlations at $z = 2.3$ with SDSS DR12 Ly α -Forests, *Astron. & Astrophys.* 603 (2017) A12. [arXiv:1702.00176](#).
- [52] M. Moresco, L. Pozzetti, A. Cimatti, R. Jimenez, C. Maraston, L. Verde, D. Thomas, A. Citro, R. Tojeiro, D. Wilkinson, A 6% measurement of

the Hubble parameter at $z \sim 0.45$: direct evidence of the epoch of cosmic re-acceleration, *J. Cosmology and Astroparticle Physics* 5 (2016) 014.
[arXiv:1601.01701](https://arxiv.org/abs/1601.01701).